J Mater Sci (2011) 46:1857–1861
DOI 10.1007/s10853-010-5013-3

Polyaniline/multiwall carbon nanotube nanocomposite for detecting aromatic hydrocarbon vapors

Wei Li · Dojin Kim

Received: 5 September 2010 / Accepted: 15 October 2010 / Published online: 26 October 2010

Abstract In this paper, polyaniline/multiwall carbon nanotube (PANI/MWCNT) composites were fabricated through an in situ polymerization method and were applied for the detection of aromatic hydrocarbon vapors. The composites were characterized by scanning electron microscopy (SEM), Fourier transform infrared spectroscopy, and Raman spectroscopy. The SEM results showed that the PANI was uniformly coated on the MWCNT, and the coating thickness was dependent on the mass ratio of aniline monomer to MWCNT. The response to aromatic hydrocarbon vapors was investigated in several hundreds ppm ranges. The sensor showed an increase in conductivity, and the maximum response measured at 1000 ppm was several tens of percent.

Introduction

Aromatic hydrocarbons are important solvents and precursors used in synthetic chemistry. They are also well recognized as serious hazards both to the environment and to human health. For example, according to the World Health Organization (WHO), benzene has an adverse effect on human blood, immunity, reproduction, genes, and so on [1]. Hence, appropriate sensors are required in working environments to warn of aromatic hydrocarbon exposures before they jeopardize the safety of workers. However, so far, the comprehensive studies on chemiresistive sensors able to detect aromatic hydrocarbon vapors are very few in comparison with those on inorganic gases, such as NH_3, H_2, CO, and NO.

Presently, the preparation of nanocomposites involving the combination of carbon nanotube (CNT) and conducting polymers has received considerable attention. The combination of CNT and conducting polymers is expected to merge and enhance the unique properties of each component and to conquer effectively the limitation of the poor interaction between the pristine nanotube and gas molecule [2, 3]. Of the family of conducting polymers, polyaniline (PANI) is perhaps the most intensively studied due to its high environmental stability, stable electrical conduction, and unique acid/base doping/dedoping chemistry. A number of studies on PANI/CNT composite gas sensors have been reported in the past several years [3–7]. To the best of our knowledge, however, no comprehensive reports on a PANI/CNT composite being used as sensor for aromatic hydrocarbon vapors has been published. As these organic vapors are fatal to both humans and the environment, there is a need to develop a reliable sensor to detect them. Therefore, a study on polyaniline/multiwall carbon nanotube (PANI/MWCNT) composites for the detection of aromatic hydrocarbon vapors was carried out and presented in this paper.

Experimental procedure

Materials

Highly purified MWCNTs (>95%) with diameter of 60–90 nm were purchased from NanoKarbon Co. Ltd., Korea. All chemicals and solvents of the highest commercially available purity were purchased from Sigma–Aldrich and were used without further purification.

W. Li · D. Kim (✉)
Department of Material Science and Engineering,
Chungnam National University, Daejeon, Korea
e-mail: dojin@cnu.ac.kr

Preparation of PANI/MWCNT composite

The composite samples were prepared by in situ polymerization methods of aniline in the presence of MWCNT. In detail, aniline monomer (An) and MWCNT were added to 50 mL of 1 M HCl solution, while ammonium persulfate (APS, >98+%, A.C.S. reagent) was dissolved in another 50 mL of 1 M HCl solution. The mass ratios of aniline monomer and MWCNT were varied; An:MWCNT = 1:4, 1:1, and 4:1. Oxidative polymerization was carried out at room temperature. The APS solution was quickly added to the An/MWCNT solution and was stirred for 2 h. The resulting solution was filtered with filter paper, and the product was washed with a large amount of deionized water.

Characterization

The surface morphology of the synthesized PANI nanofibers was examined by scanning electron microscopy (SEM: JEOL-7000) at an accelerating voltage of 15 kV. Fourier transformed infrared (FT-IR) spectrum was recorded with a Bio-Rad FTS-175C within the scanning range of 500–4500 cm^{-1}. Raman measurements were made in backscattering geometry with a JY LabRam HR fitted with a liquid-nitrogen cooled CCD detector. The spectra were collected under ambient conditions using the 514.5 nm line of an argon-ion laser with a power of 0.5 mW.

Sensor property measurements

The gas-sensing properties were measured to aromatic hydrocarbon vapors in a stainless steel chamber equipped with a temperature controlled chuck. Mass flow controllers were used to regulate separate flows of dry air and aromatic hydrocarbon vapors. The concentration calculation can be found in previous report of ours [8]. The current flowing through the sensor was monitored with time at a given voltage applied by a source-meter, Keithley Model 2400. The sensor was investigated at room temperature. The sensor response S was defined by R/R_o, where R_o is the initial stand-by resistance of the sensor, and R is the resistance when exposed to the aromatic hydrocarbon vapors.

Results and discussion

Figure 1 shows the SEM images of the PANI/MWCNT composites. The image of MWCNT is also presented for comparison. A tubular layer of PANI is uniformly coated on the surface of MWCNT. These composite are typical

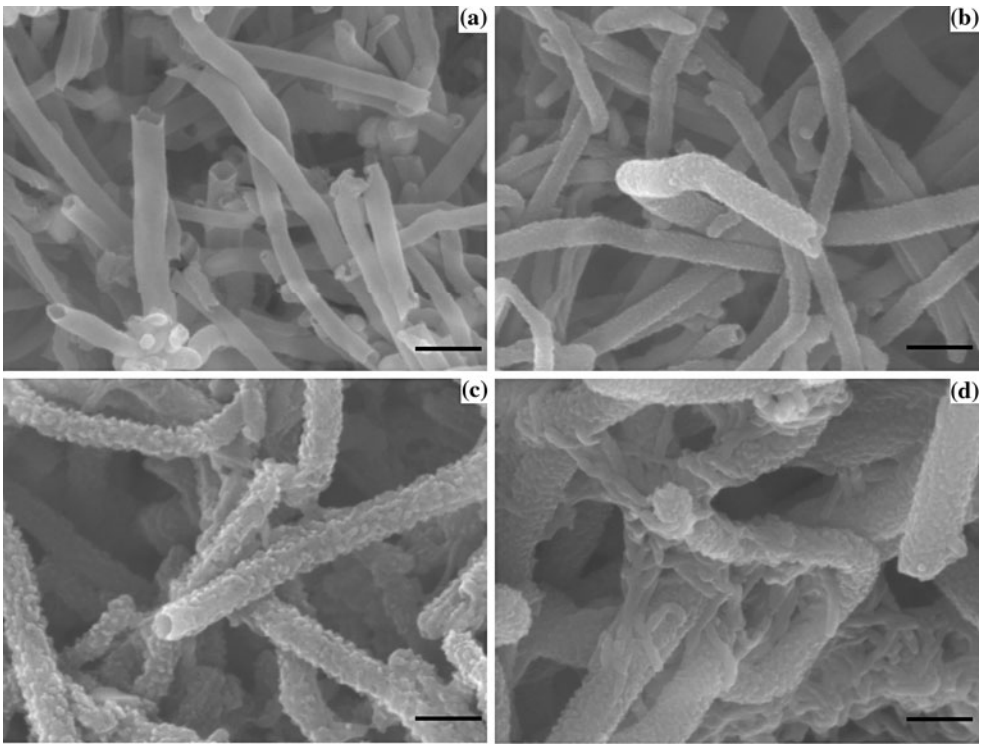

Fig. 1 SEM images of MWCNT and PANI/MWCNT composites: **a** MWCNT, **b** PANI/MWCNT (1:4), **c** PANI/MWCNT (1:1), **d** PANI/MWCNT (4:1). The *scale bar* in each picture is 200 nm

core–shell structures in which the MWCNT serves as the core and is dispersed individually into the PANI matrix [9]. The diameter of the tubular PANI/MWCNT composite is dependent on the mass ratio of An:MWCNT and is larger than that of pure MWCNT. Furthermore, some nanotubes with a diameter of ~20 nm are in Fig. 1d. Their diameter is smaller than that of pure MWCNTs but belong to the range of pure PANI nanofibers [10]. It has been deduced that the formation of these pure PANI nanofibers is due to the high mass ratio of An:MWCNT (4:1), where some aniline monomers can directly form nanofibers instead of polymerizing on MWCNT.

The FT-IR spectra of PANI and the PANI/MWCNT composites are shown in Fig. 2. The FT-IR spectra reveal distinct peaks at 1560, 1470, 1290, and 1110 cm^{-1}, which are all typical vibration modes of PANI. The absorption peaks at 1560 and 1470 cm^{-1} are assigned to the C–C stretching modes of quinoid and benzenoid rings, respectively. The relative intensity of the two peaks implies comparison of the relative amount of each oxidation state in the PANI [8]. The compatible intensity of the two peaks indicates a compatible amount of quinoid and benzenoid rings as the emeraldine oxidation state of the PANI. The peak at 1290 cm^{-1} is interpreted as the stretching vibration of the C–N bond while the peak at 1110 cm^{-1} is the in-plane C–H bending mode. The appearance of the latter peak also indicates the emeraldine oxidation state of the PANI or a highly doped PANI. In addition, a notable increase in the intensity ratio of the quinoid to benzenoid ring is observed for the PANI/MWCNT composites. This phenomenon is commonly observed in PANI/MWCNT composites prepared by the in situ process in the comparison with pure emeraldine salt form PANI [11]. This may also indicates that the interaction between PANI and MWCNT is π-stacking, which can take place between the π-bonded surface of MWCNT and the quinoid ring of PANI [12]. Moreover, according to the research of MacDiarmid et al., the quinoid peak is a measure of the degree of delocalization of the electrons, and the increase in the relative intensity indicates an increase in the effective degree of electron dislocation [13].

Raman spectra as complementary investigation to FT-IR are given in Fig. 3. The typical peaks at 1170, 1245, 1331, 1500, and 1627 cm^{-1} correspond to the PANI vibration modes. The peaks at 1170 and 1245 cm^{-1} are the C–H bending of quinoid and benzenoid rings, respectively. The peaks at 1331 and 1500 cm^{-1} are interpreted as the C–N^+ and C=N stretching vibrations, respectively. The peak at 1627 cm^{-1} is the C–C stretching of benzene ring. These stretching vibration modes reveal the presence of a highly doped PANI [14]. For the PANI/MWCNT composites, the Raman spectra reveal two distinct peaks related to the MWCNT vibration modes. The peak at 1590 cm^{-1}, a so-called G-band, corresponds to the sp^2 vibration of a 2D hexagonal lattice in the graphite. Another peak at 1350 cm^{-1}, the so-called D-band, is related to glassy carbon or disordered graphite. However, this D-band is not observed in Fig. 3. It may have overlapped with the nearby C–N^+ stretching vibration (1331 cm^{-1}) of PANI [9].

As the objective of this experiment is to obtain novel synergetic outputs by combining two components, it is necessary to investigate the effect of the mass ratio of the composites on the sensor behaviors. Figure 4 shows the sensor response at room temperature to one of typical

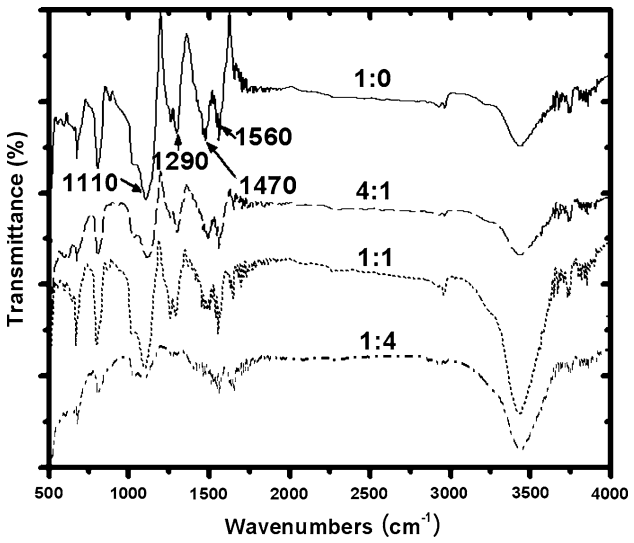

Fig. 2 FT-IR spectra of PANI/MWCNT composites with different mass ratios: 1:0 (*solid line*), 4:1 (*dashed line*), 1:1 (*dotted line*), 1:4 (*dash-dotted line*)

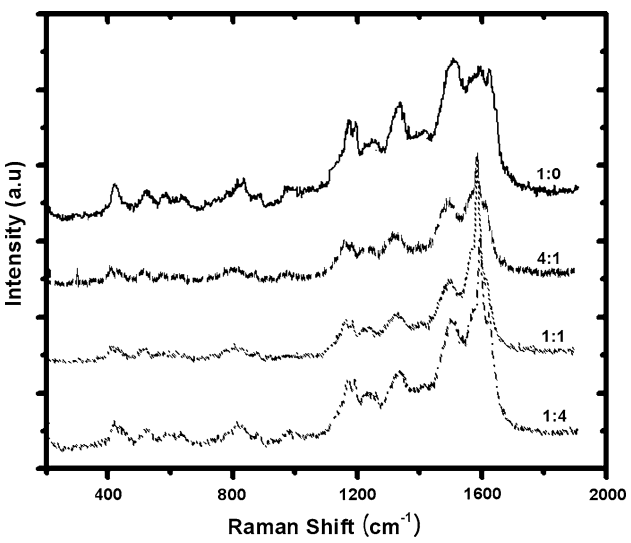

Fig. 3 Raman spectra of PANI/MWCNT composites with different mass ratios: 1:0 (*solid line*), 4:1 (*dashed line*), 1:1 (*dotted line*), 1:4 (*dash-dotted line*)

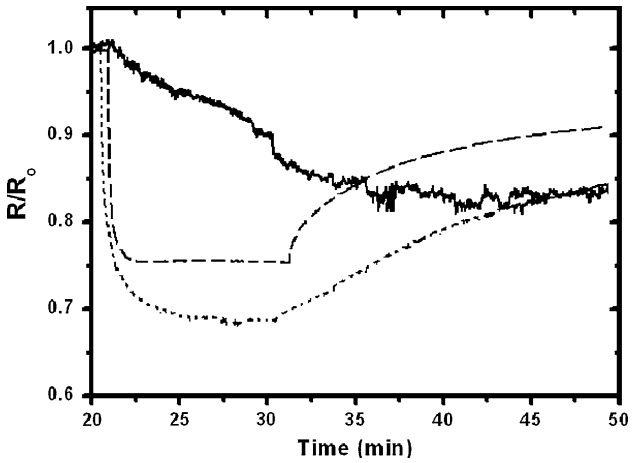

Fig. 4 Response to 1000 ppm *o*-xylene of PANI/MWCNT with different mass ratios: 1:4 (*solid line*), 1:1 (*dashed line*), and 4:1 (*short dashed line*)

aromatic hydrocarbon vapors, *o*-xylene. The response of the sensors markedly is reduced upon increasing the MWCNT content. Similar results have also been reported by Ma et al. [4] when they used PANI/MWCNT composites for detecting trimethylamine vapors. The high response of PANI/MWCNT (4:1) is due to its high degree of electron delocalization which leads to high charge transfer.

The sensor response upon varying the vapor concentration from 200 to 1000 ppm is shown in Fig. 5, and seems to be well proportioned to the vapor concentration. Moreover, the response increases in the order of polarity of the molecules. For instance, the maximum resistance change at 1000 ppm benzene, toluene, *p*-xylene, *m*-xylene, *o*-xylene, and ethylbenzene is 0.11, 0.15, 0.20, 0.21, 0.31, and 0.26, respectively, while the dipole moment of benzene, toluene, *p*-xylene, *m*-xylene, *o*-xylene, and ethylbenzene is 0, 0.37, 0.07, 0.31, 0.65, and 0.59 D, respectively [15]. The dipole moments of the aromatic hydrocarbon vapors are related to the response level of PANI nanofibers [8]. The core–shell structure of the PANI/MWCNT composite allows it to reproduce this polarity-dependent property upon exposure to aromatic hydrocarbon vapors. The dipole moment of a polar aniline monomer is 1.13 D, which is much higher than that of other aromatic hydrocarbon vapors. The polar groups (–NH) on the polymer chain can induce dipoles in the adjacent non-polar aromatic hydrocarbon molecules, and a weak bond can form as a result of the attractive force. Figure 6 shows the typical responding behaviors of the PANI/MWCNT composite sensor upon repeated exposure to some aromatic hydrocarbon vapors. The recovery is very poor at room temperature, which is probably due to the introduction of MWCNT, as discussed below.

Although conducting polymer sensor is widely studied for the detection of organic vapors, such as methanol [16], chloroform [17], toluene [18], acetone [19], and others, the interaction mechanism with these organic vapors is still not fully understood, and some controversial results can be found [18, 19]. On the other hand, that relatively non-reactive organic compounds physically interact with conducting polymers is generally agreed upon [20]. In addition, based on our recent report on an X-ray photoelectron spectroscopy (XPS) study of the electronic state of PANI [8], the conductivity change in PANI upon exposure to aromatic molecules is related to physical interaction instead of chemical interaction. Such physical interaction due to dipole-(induced) dipole force may uncoil the polymer chains and decrease the hopping distance for the charge carriers.

Although MWCNTs are fully wrapped in PANI matrix, their interaction with aromatic molecules can still be

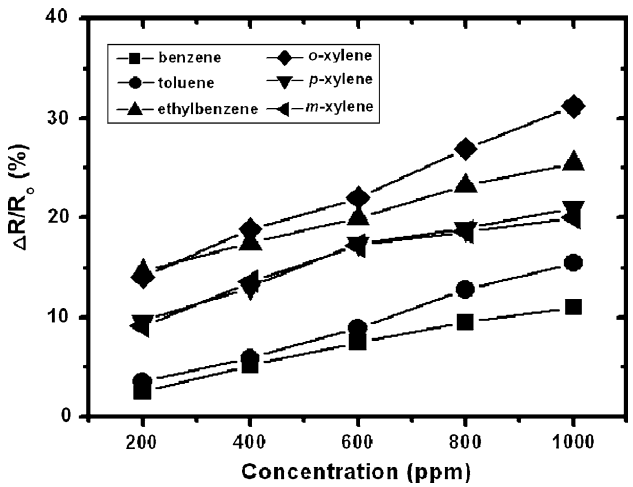

Fig. 5 Resistance change of PANI/MWCNT (4:1) composite versus vapor concentration

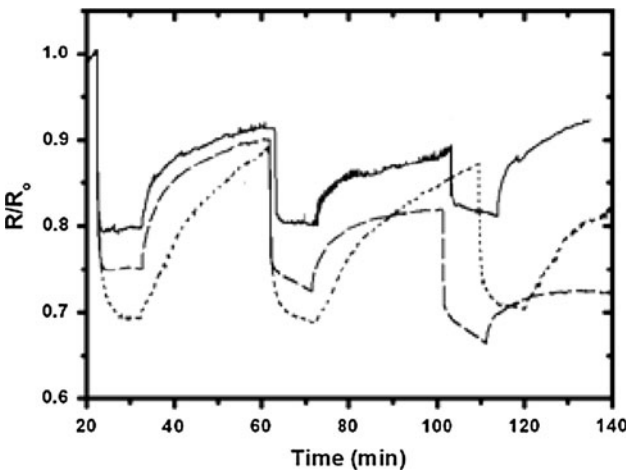

Fig. 6 Response of PANI/MWCNT (4:1) composite upon repeat exposure to 1000 ppm *p*-xylene (*solid line*), ethylbenzene (*dashed line*), and *o*-xylene (*short dashed line*)

expected to occur because PANI has an interchain distance of ~0.9 nm [21, 22] which should be accessible for small size aromatic molecules (~0.7 nm) [15]. According to the researches of Gauden et al. [23] and Shi et al. [24], there are two types of benzene molecules in nanotubes: those within CNTs (intra-benzene) and those on the surface of CNTs. The amount of intra-benzene is significantly higher in an opened MWCNT (opened tip, Fig. 1a) than in as-received MWCNTs (closed tip). These amounts of intra-benzene also have larger entropy values than the molecules located on the surface of the nanotube [23, 25], which may result in the poor recovery of composite compared with that observed in pure PANI [8].

Conclusions

PANI/MWCNT composite has been successfully prepared by in situ polymerization method. The CNTs are fully wrapped within the PANI matrix to form a core–shell structure. The interaction between PANI and CNT is π-stacking interaction, which can increase the conductivity but reduce the magnitude of sensor response. The interaction between aromatic molecules and PANI/MWCNT composites is non-covalent or physical interaction. The poor recovery of the composite may be related to the difficult desorption of intra-benzene rings.

Acknowledgement This work was supported by the National Laboratory Research Program, Korea.

References

1. World Health Organization, Effect of benzene on air indoor quality, www.euro.who.int/document/aiq/5_2benzene.pdf. Accessed 8 Apr 2010
2. Sainz R, Small WR, Young NA, Vallés C, Benito AM, Maser WK, Panhuis M (2006) Macromolecules 39:7324
3. Chang Q, Zhao K, Chen X, Li M, Liu J (2008) J Mater Sci 43:5861. doi:10.1007/s10853-008-2827-3
4. Ma X, Zhang X, Li Y, Li G, Wang M, Chen H, Mi Y (2006) Macromol Mater Eng 291:75
5. Zhang T, Nix MB, Yoo BY, Deshusses MA, Myung NV (2006) Electroanalysis 18:1153
6. He L, Jia Y, Meng F, Li M, Liu J (2009) Mater Sci Eng B 16:76
7. Chang CP, Yuan CL (2009) J Mater Sci 44:5485. doi:10.1007/s10853-009-3766-3
8. Li W, Nguyen DH, Cho Y, Kim D, Kim J (2009) Sens Actuators B 143:132
9. Wu T, Lin Y (2006) Polymer 47:3576
10. Ding H, Wan M, Wei Y (2007) Adv Mater 19:465
11. Yan X, Han Z, Yang Y, Tay B (2007) J Phys Chem C 111:4125
12. Baibarac M, Baltog I, Lefrant S, Mevellec JY, Chauvet O (2003) Chem Mater 15:4149
13. Quillard S, Louarn G, Lefrant S, MacDiarmid AG (1996) Phys Rev B 50:12496
14. Louarn G, Lapkowski M, Quillard S, Pron A, Buisson JP, Lefrant S (1996) J Phys Chem 100:6998
15. Lide DR (2005) Handbook of chemistry and physics. CRC Press, Boca Raton
16. Tan CK, Blackwood DJ (2000) Sens Actuators B 71:184
17. Virji S, Huang J, Kaner RB, Weiller BH (2004) Nano Lett 4:491
18. Roh JG, Hwang HR, Yu JB, Lim JO, Huh JS (2002) J Macromol Sci A 39:1095
19. Kim JS, Sohn SO, Huh JS (2005) Sens Actuators B 108:409
20. Lange U, Roznyatovskaya NV, Mirsky VM (2008) Anal Chim Acta 614:1
21. Zhu C, Wang C, Yang L, Bai C, Wang F (1999) Appl Phys A 68:435
22. Pouget JP, Jozefowicz ME, Epstein AJ, Tang X, MacDiarmid AG (1991) Macromolecules 24:779
23. Gauden PA, Terzyk AP, Rychlicki G, Kowalczyk P, Lota K, Raymundo-Pinero E, Frackowiak E, Béguin F (2006) Chem Phys Lett 421:409
24. Shi W, Johnson JK (2003) Phys Rev Lett 91:015504
25. Tournus F, Latil S, Heggie MI, Charlier JC (2005) Phys Rev B 72:075431